Sf 298 MASTER COPY KEEP THIS COPY FOR REPORDUCTION PURPOSES

REPORT DOCUMENTATION PAGE

Form Approved OMB NO. 0704-0188

Public reporting burden for this collection of information is estimated to average 1 hour per response, including the time for reviewing instructions, searching existing data sources, gathering and mainttaining the data needed, and completing and reviewing the collection of information. Send comment regarding this burden exti8mates or any other aspect of this collection of information, including suggestions for reducing this buren, to Washington Headquarters Services, Directorate for Information Operations and Reports, 1215 Jefferson Davis Highway, Suite 1204, Arlington VA 22202-4302, and to the Office of Management and Budget, Paperwork Reduction Project (0904-0188) Washington, DC 20503

1. AGENCY USE ONLY *(Leave Blank)*

2. REPORT DATE
February 29, 2000

3. REPORT TYPE AND DATES COVERED
Final, 9/1/96 - 2/29/00

4. TITLE AND SUBTITLE
Computer Simulation of Strain Engineering and Phononics in Semiconducting Nanostructures on Parallel Architectures

5. FUNDING NUMBERS
DAAH04-96-1-0393

6. AUTHOR(S)
Aiichiro Nakano, Rajiv K. Kalia, and Priya Vashishta

7. PERFORMING ORGANIZATION NAMES(S) AND ADDRESS(ES)
Louisiana State University
Concurrent Computing Laboratory for Materials Simulations
Coates Hall, Baton Rouge, Louisiana 70803-4020

8. PERFORMING ORGANIZATION REPORT NUMBER

9. SPONSORING/MONITORING AGENCY NAME(S) AND ADDRESS(ES)
U.S. Army Research Office
P.O. Box 12211
Research Triangle, NC 27709-2211

10. SPONSORING/MONITORING AGENCY REPORT NUMBER
ARO 36347.17-EL-DPS

11. SUPPLEMENTARY NOTES
The views, opinions and/or finding in this report are those of the author(s) and should not be construed as an official Department of the Army position, polity or decision, unless so designated by other documentation.

12a. DISTRIBUTION/AVAILABILITY STATEMENT
Approved for public release; distribution unlimited.

12b. DISTRIBUTION CODE

13. ABSTRACT *(Maximum 200 words)*

Feature sizes of semiconductor devices are expected to shrink to 70 nm in the next 10 years in order to achieve higher processing speed and memory density. In the sub-0.1-µm regime, a number of critical issues require atomistic modeling.

Large-scale parallel molecular dynamics (MD) simulations have been performed to investigate: fracture in GaAs thin films; structural transformation in GaAs nanocrystals; structural, mechanical, and vibrational properties of GaAs/InAs alloys for optoelectronic applications; inhomogeneous stress distribution in Si/Si_3N_4 nanopixels; oxidation dynamics of aluminum nanoclusters; and dielectric properties of high-permittivity TiO_2 for ultrathin gate dielectric films. Scalable software infrastructure has been developed to enable multiscale simulations of nanoelectronic devices using MD and quantum mechanical methods.

Currently, MD simulations are being performed to investigate stress-driven self-limiting growth of InAs nanomesas on GaAs and nanoindentation for mechanical realiability of nanoelectronic devices.

20001122 087

14. SUBJECT TERMS

15. NUMBER IF PAGES

16. PRICE CODE

17. SECUIRTY CLASSIFICATION OR REPORT	18. SECURITY CLASSIFICATION OF THIS PAGE	19. SECURITY CLASSICATION OF ABSTRACT	20. LIMITATION OF ABSTRACT
UNCLASSIFIED	UNCLASSIFIED	UNCLASSIFIED	UL

NSN 7540-01-280-5500

Standard Form 298 (Rev. 2-89)
Prescribed by ANSI Std 239-18

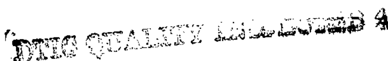

TABLE OF CONTENTS

COVER SHEET i

TABLE OF CONTENTS ii

§1 ACCOMPLISHMENTS 1

§1.1 FRACTURE IN GaAs 1

§1.2 STRUCTURAL TRANSFORMATION IN GALLIUM ARSENIDE NANOCRYSTALS 2

§1.3 STRUCTURAL, MECHANICAL, AND VIBRATIONAL PROPERTIES OF GaAs/InAs ALLOYS 4

§1.4 STRESS IN Si/Si_3N_4 NANOPIXELS 6

§1.5 OXIDATION OF ALUMINUM NANOCLUSTERS 6

§1.6 DIELECTRIC PROPERTIES OF HIGH-*k* MATERIALS 7

§1.7 MULTILEVEL ALGORITHMS FOR PARALLEL MOLECULAR DYNAMICS SIMULATIONS 8

§2 RESEARCH IN PROGRESS 9

§2.1 STRESS DISTRIBUTION IN InAs/GaAs MESAS 9

§2.2 NANOINDENTATION IN Si_3N_4 SURFACES 10

§2.3 SCALABLE MOLECULAR-DYNAMICS/QUANTM-MECHANICAL ALGORITHMS 11

§2.4 HYBRID MOLECULAR-DYNAMICS/QUANTM-MECHANICAL SIMULATION APPROACH 12

§3 INTERACTIONS 13

§4 TRAINING OF GRADUATE STUDENTS 13

§5 COMPUTATIONAL FACILITIES 14

§6 PUBLICATIONS 15

§7 SCIENTIFIC PERSONNEL 18

§8 INVENTIONS 18

§1 ACCOMPLISHMENTS

Feature sizes of semiconductor devices are expected to shrink to 70 nm in the next 10 years in order to achieve higher processing speed and memory density. In the sub-0.1-μm regime, a number of critical issues require atomistic modeling. First, macroscopic material properties often do not hold at the nanometer scale. For example, a SiO_2 film no longer acts as an insulator with thickness less than 0.7 nm. In order to reduce the leakage currents in gate dielectric films, higher-permittivity materials are being sought to replace SiO_2. These so called high-k materials include silicon oxynitrides and TiO_2 among others. Another critical issue is inhomogeneous nature of structural, mechanical, and vibrational properties at atomic scales in lattice-mismatched alloys such as GaAs/InAs, which must be taken into consideration for mechanical and thermal stability of nanoelectronic structures.

Stress also plays a critical role in the fabrication of nanoscale devices by interfacet adatom migration on patterned surfaces and lattice-mismatch-stress induced growth of coherent 3D islands. Atomistic simulations are expected to guide the design of optimal surface patterns for nanodevice fabrication.

Physical properties of nanometer-size structures often exhibit significant size dependence. Examples include phase stability and oxidation reaction. Variation of physical properties with size could provide methods for designing devices with controlled properties.

During the three and a half years of this project, large-scale (10-100 million atoms) parallel molecular dynamics (MD) simulations have been performed to study a number of physical properties and processes in nanometer-size structures:

1. Fracture in GaAs thin films (§1.1);
2. Structural transformation in GaAs nanocrystals (§1.2);
3. Structural, mechanical, and vibrational properties of GaAs/InAs alloys (§1.3);
4. Inhomogeneous stress distribution in Si/Si_3N_4 nanopixels (§1.4);
5. Oxidation dynamics of aluminum nanoclusters (§1.5);
6. Dielectric properties of high-k TiO_2 (§1.6).

These large-scale atomistic simulations have been enabled by combining novel parallel multilevel algorithms and new simulation methodologies including a variable-charge MD approach, see §1.7.

These research activities resulted in 46 refereed publications (see §6).

§1.1 FRACTURE IN GaAs

Energetics of surface microstructures (steps, kinks, and mesas) is of essential importance for the fabrication of semiconductor devices. Surface energies of GaAs and other semiconductors have been derived from fracture experiments. Fracture energy measured in these experiments, however, involves various dissipation terms (such as dislocation emission and void nucleation) in addition to the energy for cleavage debonding.

A fundamental quantity involved in fracture is the energy release rate, G—the rate at which the mechanical energy stored in the elastic body flows into the crack tip per unit crack advance. It is the energy to create a new surface of unit area during fracture process, and consists of the energy for cleavage debonding and any associated energy dissipations. G_c is the minimum energy at which crack propagation is possible, and it is an intrinsic material property that characterizes toughness.

Molecular-dynamics simulations involving up to 100 million atoms have been performed to study fracture in GaAs thin-film strips, see Fig. 1. Significant orientation dependence of fracture is observed (Fig. 2). (110) fracture is cleavage-like and is characterized by $G_c = 1.4 \pm 0.1$ J/m^2. The

calculated critical energy release rate agrees well with available experimental data, 1.5 - 1.7 J/m^2. In contrast to the cleavage-like (110) fracture, (111) fracture involves slip in the $(11\bar{1})$ plane, and crack branching is observed in (001) fracture. Accordingly, these surfaces are characterized by larger toughness values: G_c = 1.7 J/m^2 for (111) and G_c = 2.0 J/m^2 for (001).

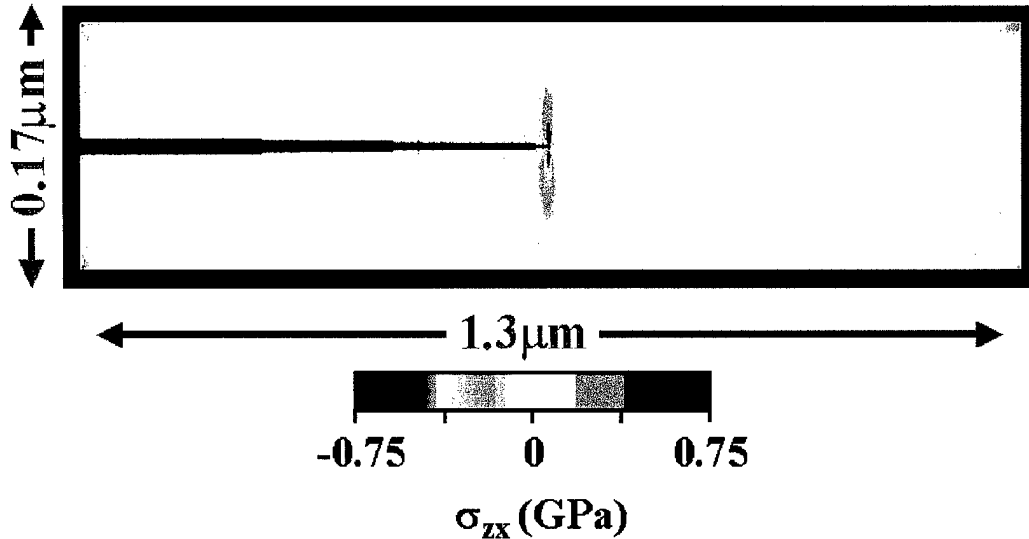

Fig. 1: Shear stress distribution near a crack tip in a GaAs thin-film strip consisting of 100-million atoms.

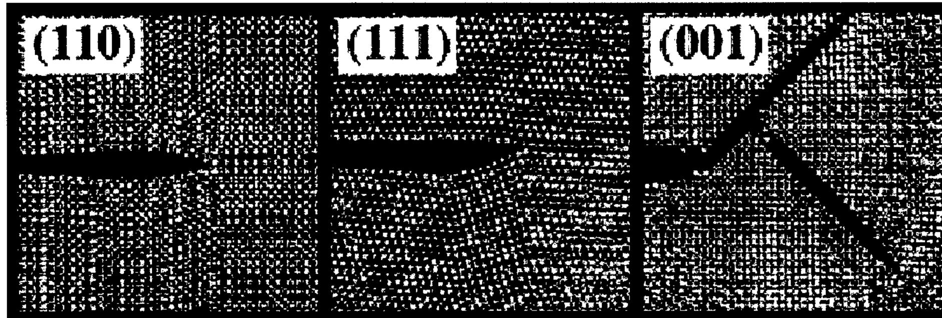

Fig. 2 : Atomic configurations near crack tips in GaAs for (110), (111), and (001) fracture surfaces.

§1.2 STRUCTURAL TRANSFORMATION IN GALLIUM ARSENIDE NANOCRYSTALS

Despite numerous experimental and theoretical studies, structural transformations in GaAs and SiC at high pressures are not well understood at the atomistic level. We have investigated the mechanisms of these transformations using an isothermal-isobaric MD approach and new interatomic potential schemes. In SiC, a reversible transformation between the four-fold coordinated zinc-blende structure and the six-fold coordinated rocksalt structure is found at a pressure of 100 GPa. The calculated volume change at the transition and the hysteresis are in good agreement with experimental data. The atomistic mechanism for the structural transformation is a cubic-to-monoclinic unit-cell transformation and a relative shift of Si and C sublattices in the [100] direction. The new transition path does not involve any bond breaking and it has a significantly lower activation energy compared with a previously proposed transformation mechanism (Fig. 3).

In crystalline GaAs, the pair-distribution functions and bond-angle distributions indicate that the four-fold coordinated zinc-blende structure transforms into a six-fold coordinated orthorhombic structure at a pressure of 22 GPa. The reverse transformation from the orthorhombic to zinc-blende structure shows hysteresis and is observed at a pressure of ~ 10 GPa. These MD

results are in good agreement with experiments (Fig. 4). The calculated volume change of ~ 16% is also in agreement with experiments.

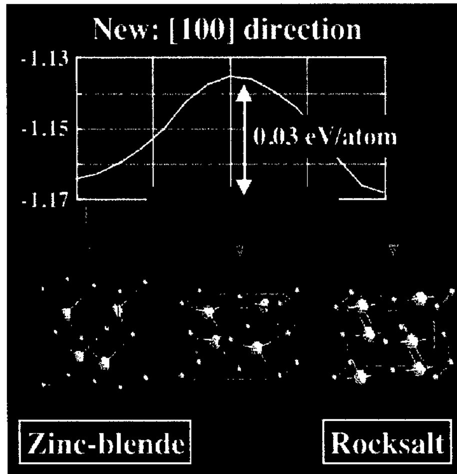

Fig. 3: The newly proposed transition path for the pressure-induced zinc-blende-to-rocksalt transformation in SiC involves a relative shift of Si and C sublattices in the [100] direction. It has a small activation enthalpy (0.03 eV/atom).

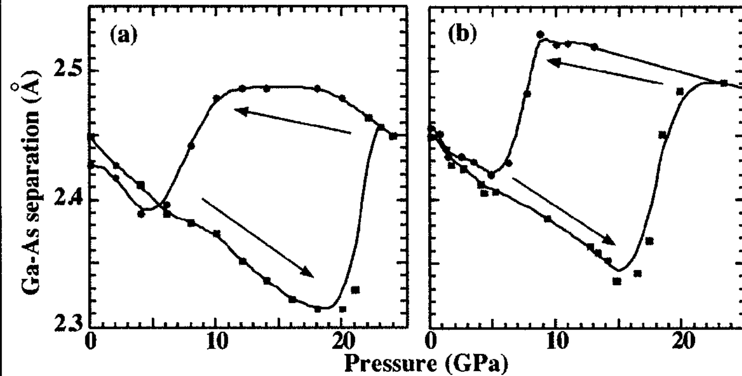

Fig. 4: Comparison between (a) MD and (b) EXAFS experimenta results [J. M. Besson, J. P. Itie, A. Polian, *et al.*, Phys. Rev. B **44**, 4214 (1991)] for the Ga-As nearest-neighbor distance during forwar (squares) and reverse (circles) structural transformations.

Aggregates of nanometer-size semiconductor crystals have promising applications as photovoltaics, light-emitting diodes, and single-nanocrystal, single-electron transistors.* We have investigated pressure-induced structural transformations in GaAs nanocrystals of different sizes using parallel MD simulations. It is found that the transformation from four-fold (zinc blende) to six-fold coordination starts at the surfaces of nanocrystals and proceeds inwards with increasing pressure. Inequivalent nucleation of the high-pressure phase at different sites leads to an inhomogeneous deformation of the nanocrystal. For sufficiently large spherical nanocrystals, this gives rise to rocksalt structures of different orientations separated by grain boundaries, see Fig. 5. The absence of such grain boundaries in a faceted nanocrystal of moderate size indicates sensitivity of the transformation to the initial nanocrystal shape. The pressure corresponding to the complete transformation increases with the nanocrystal radius and it approaches the bulk value for a spherical nanocrystal of ~ 5,000 atoms.

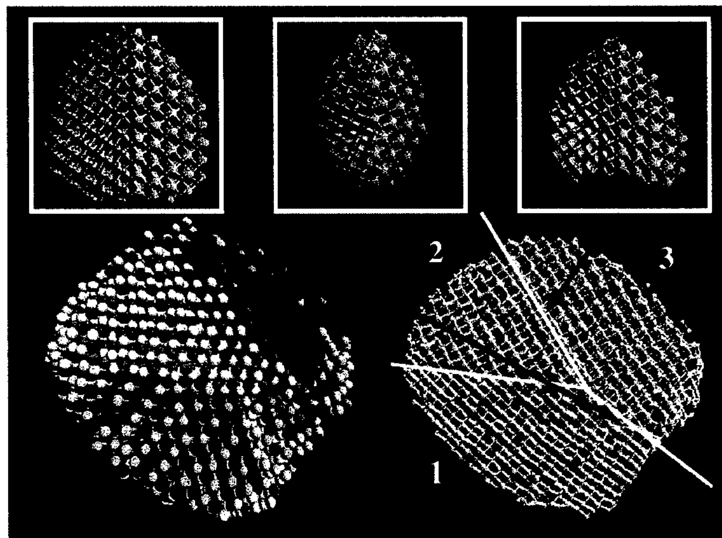

Fig. 5: Bottom left panel shows color-coded grain structures in a GaAs nanocrystal at a pressure of 22.5 GPa. Bottom right panel and insets show different grain boundary types.

*J. N. Wickham, A. B. Herhold, and A. P. Alivisatos, Phys. Rev. Lett. **84**, 923 (2000).

§1.3 STRUCTURAL, MECHANICAL, AND VIBRATIONAL PROPERTIES OF GaAs/InAs ALLOYS

Reliable interatomic potential is an essential ingredient of MD simulations to investigate the atomic-level surface stresses, surface stoichometry and migration processes, and the mechanical stresses in lattice-mismatched InAs/GaAs systems. A significant step forward was taken in developing an interatomic potential for GaAs and InAs. The potential was validated against experimental data and first-principles bulk electronic structure calculations on pressure-induced structural transformations, melting/recrystallization, and the cleavage energy. Phonon dispersion of GaAs also agrees well with experimental data (Fig. 6). The MD results for the LO (longitudinal optical)-TO (transverse optical) phonon energy splitting at the Γ point, 2.85 meV for GaAs and 2.46 meV for InAs, are also in reasonable agreement with experimental data (2.70 meV for GaAs and 2.46 meV for InAs, respectively).

In addition to describing bulk crystal properties, the interatomic potentials provide excellent representation of amorphous systems. For example, static structure factor of amorphous GaAs is in excellent agreement with neutron scattering data, see Fig. 7.

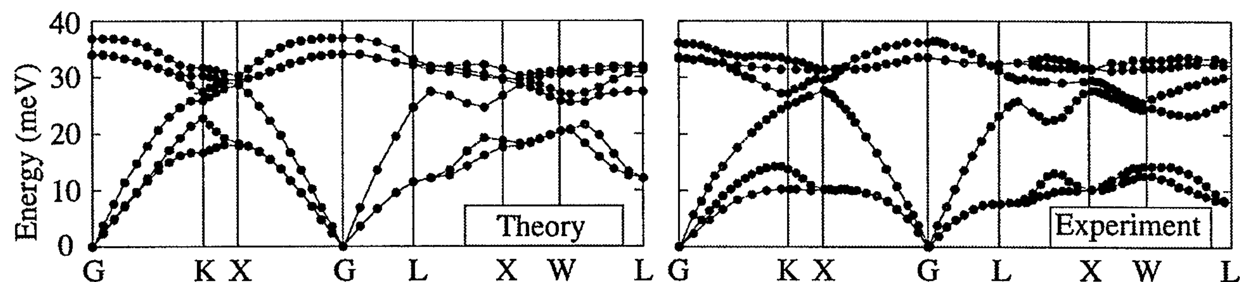

Fig. 6: Theoretical and experimental [D. Strauch and B. Dorner, J. Phys.: Condens. Matter **2**, 1457 (1990)] phonon dispersion of zinc-blende GaAs.

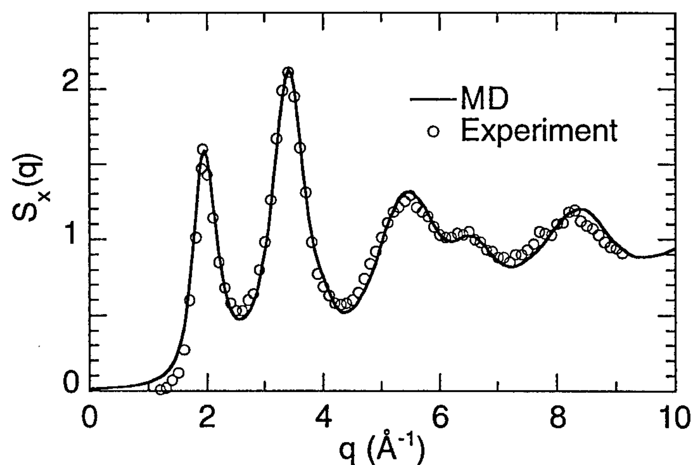

Fig. 7: X-ray static structure factor of amorphous GaAs at density 5.11 g/cm^3. The solid curve and circles represent MD and experimental [D. Udron *et al.*, J. Non-Cryst. Solids **137&138**, 131 (1991)] data, respectively.

In order to study InAs/GaAs mesas, we need to develop an interatomic-potential scheme for mixed InAs/GaAs systems. Recently, we have developed a scheme to combine interatomic potentials of binary materials in such a way that the resulting potential depends on the local chemical environment. For systems involving Ga, In, and As, we use a linear mixing scheme to combine the interatomic potentials for GaAs and InAs. This scheme is adaptive in which As atoms are classified into different types according to the number of Ga and In neighbor atoms.

To validate this scheme, we have performed MD simulations to calculate the structural correlation in $Ga_{1-x}In_xAs$ alloy. Both GaAs and InAs form the zinc-blende structure at low pressures. Due to the lattice mismatch, the volume of $Ga_{1-x}In_xAs$ alloy is an increasing function of x. However, both Ga-As and In-As bond lengths change very little as a function of x, as observed in the EXAFS (extended x-ray absorption fine structure) experiments in Fig. 8. These behaviors of the bond lengths are well reproduced in our MD simulations, see Fig. 8.

In pair distribution functions for cation-cation and As-As pairs obtained from MD simulations, the nearest cation-cation distance has a broad distribution, whereas the nearest As-As peak splits to into two peaks suggesting the existence of two As-As distances. This is in good agreement with experiments, and demonstrates that the second-neighbor correlation in the alloy is accurately described by MD simulations.

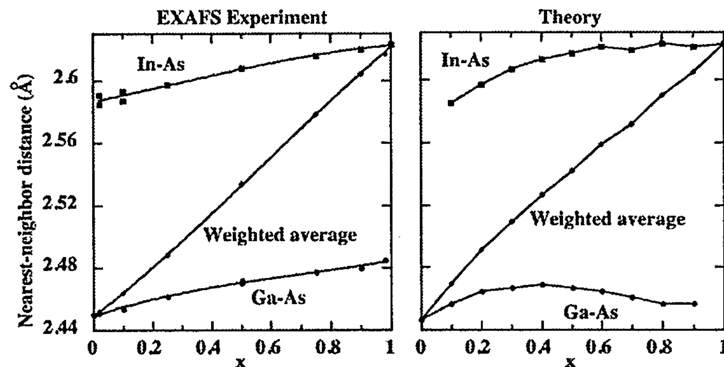

Fig. 8: (Left) EXAFS experimental data on Ga-As and In-As nearest neighbor distance as a function of alloy composition [J. C. Mikkelsen and J. B. Boyce, Phys. Rev. Lett. **49**, 1412 (1982)]. Middle curve is the virtual-crystal-approximation bond length calculated from the measured X-ray lattice constant. (Right) The MD simulation results for the same quantities.

We have used the new interatomic potential scheme to calculate the elastic constants of $Ga_{1-x}In_xAs$ alloy. The elastic constants have been found to exhibit a significant nonlinear dependence on the composition, x, see Fig. 9. We have also studied phonon density-of-states of $Ga_{1-x}In_xAs$ (Fig. 9). For intermediate x, phonon density-of-states exhibits a two-mode behavior associated with optical modes of GaAs and InAs, in agreement with recent experimental results [J. Groenen *et al.*, Phys. Rev. B **58**, 10452 (1998)].

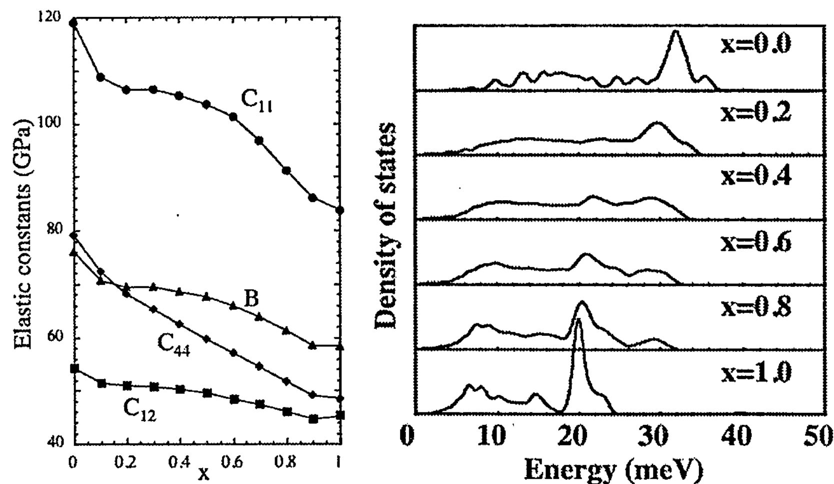

Fig. 9: (Left) Elastic constants (C_{11}, C_{12}, and C_{14}) and bulk modulus (B) of $Ga_{1-x}In_xAs$ alloy. (Right) Phonon density-of-states of the same system.

§1.4 Stress in Si/Si_3N_4 Nanopixels

We have investigated the effects of surfaces, edges, and lattice mismatch at the $Si(111)/Si_3N_4(0001)$ interface on the atomic-level stress distribution in a Si/Si_3N_4 nanopixel.

A 10-million-atom MD has been performed on 128 CPUs of the HP Examplar at Caltech. The system consists of a 539Å×32Å×10Å Si mesa which is placed on top of a 1077Å×653Å×300Å Si(111) substrate. The top surface of the mesa is covered with an 83Å-thick crystalline $Si_3N_4(0001)$ film (Fig. 10). The $Si(111)/Si_3N_4(0001)$ interface involves a 1.1% lattice mismatch inducing a stress in the system. The lattice mismatch causes compressive stresses in Si_3N_4, while a tensile stress is observed in Si. Note that edges and corners act as stress concentrators.

We have also simulated a nanopixel covered with an amorphous Si_3N_4 film. We find the stress to be highly non-uniform laterally, quite unlike those for crystalline films. Such lateral inhomogeneity in stress is expected to affect the processing of nanoscale pixels.

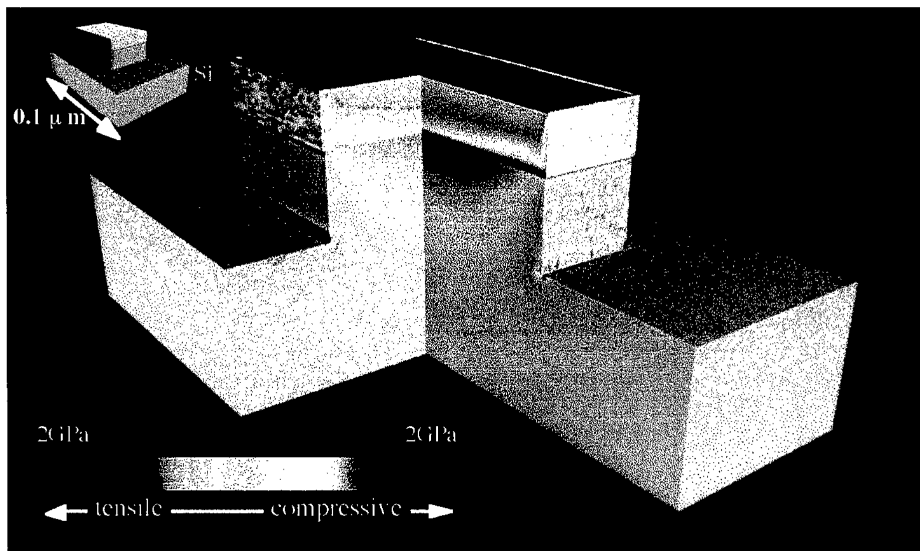

Fig. 10: Stress distribution in a Si/Si_3N_4 nanopixel consisting of 10-million atoms in the presence of the 1.1% lattice mismatch. To show the stresses inside the nanopixel one quarter of the system is removed and the value of the hydrostatic stress is color-coded.

§1.5 Oxidation of Aluminum Nanoclusters

Oxidation is important as a dielectric-layer forming process in microelectronics. Oxidation of nanometer-size clusters, however, is very different from that of large, flat surfaces. Aluminum nanoclusters of diameters 100-700 Å are known to form an oxide scale with thickness between 20 and 50 Å in low-density oxygen gases at room temperature. At high oxygen densities, however, the reaction is explosive, making Al nanoclusters an efficient rocket fuel.

We have performed the first MD simulation to study the oxidation dynamics of Al nanoclusters, see Fig. 11. An Al nanocluster of radius 100Å was placed in gaseous oxygen. The simulation takes into account the effect of dynamic charge transfer between O and Al on the basis of the electronegativity equalization principle. Oxidation starts at the surface of the cluster and the oxide layer grows to a thickness of ~35 Å. The surface oxide melts because of the high temperature due to the release of the Al-O bonding energy.

We have also performed a simulation in the canonical ensemble. An oxide scale of 40 Å thickness is subsequently formed, as seen in Fig. 12. The MD simulations provide detailed picture of the rapid evolution and culmination of the surface oxide thickness, local stresses, and atomic diffusivities. In the first 5 ps, oxygen molecules dissociate and the oxygen atoms first diffuse into

octahedral and subsequently into tetrahedral sites in the Al nanoparticle. In the next 20 ps, as the oxygen atoms diffuse radially into and the Al atoms diffuse radially out of the nanoparticle, the fraction of six-fold coordinated oxygen atoms drops dramatically. Concurrently, there is a significant increase in the number of O atoms, forming clusters of corner-sharing and edge-sharing OAl_4 tetrahedra. Between 30 and 35 ps, clusters of OAl_4 coalesce to form a neutral, percolating tetrahedral network that impedes further intrusion of oxygen atoms into and of Al atoms out of the nanoparticle. As a result, a stable oxide scale is formed. Structural analysis reveals a 40Å thick amorphous oxide scale on the Al nanoparticle. The thickness and structure of the oxide scale are in accordance with experimental results.

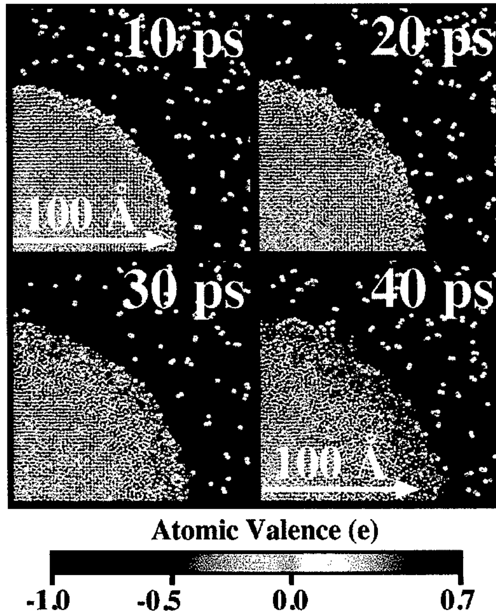

Fig. 11: Atomic charges during the oxidation of an Al nanocluster.

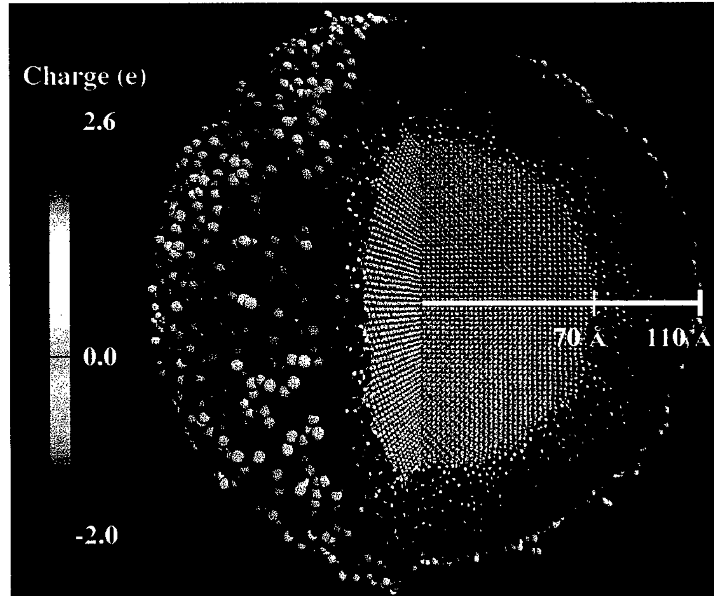

Fig. 12: Atomic charges showing an Al cluster covered with a 40 Å-thick oxide scale.

§1.6 DIELECTRIC PROPERTIES OF HIGH-*k* MATERIALS

A variable-charge MD scheme has been used to describe dielectric properties of high-*k* TiO_2. Titanium dioxide is an important ceramic for a variety of industrial applications that stem from high polarizability and large static dielectric constant (~114 for powdered rutile structure). In the vicinity of interfaces, TiO_2 exhibits significant charge fluctuations which is evident from the non-stoichiometric Ti_xO_{2x-1} (with x ranging from 4 to 10) in interfacial regions. Charge transfer among Ti and O atoms is found to be highly sensitive to the local environment, and hence the variable-charge MD is essential to describe its dielectric properties correctly.

Lattice constant, cohesive energy, and elastic moduli calculated with our new variable-charge interatomic potential are in good agreement with experimental results. The interaction potential also describes the dielectric properties of the rutile TiO_2 correctly. Static dielectric constants are calculated through the fluctuation-dissipation theorem. We consider a periodically-repeated unit cell, obtain its independent oscillatory modes by diagonalizing the dynamical matrix, and then calculate the electric dipole moment using the law of equipartition for thermal equilibrium among those modes. The dielectric constants thus calculated include the effects of ionic motion and charge transfer between atoms. (High-frequencey electronic polarization effects can be neglected, since experimental high-frequency dielectric constants, $\varepsilon_{xx}^{\infty}$=6.8 and $\varepsilon_{zz}^{\infty}$=8.4, are much smaller than their static counterparts, ε_{xx}=86 and ε_{zz}=170.) Our results for the dielectric constants, ε_{xx} = 92 and ε_{zz} = 196 agree well with experimental measurements. Pressure dependence of the dielectric constants

has also been studied. The calculated slopes, $d\ln\varepsilon_{xx}/dP = -0.09$ GPa^{-1} and $d\ln\varepsilon_{zz}/dP = -0.15$ GPa^{-1}, compare favorably with the experimental results, $d\ln\varepsilon_{xx}/dP = -0.05$ GPa^{-1} and $d\ln\varepsilon_{zz}/dP = -0.12$ GPa^{-1}. Furthermore, the calculated directionally-averaged dielectric constant of the anatase phase, 46, agrees well with an experimental value, 48. Through detailed analyses of the calculated electric-dipole oscillations, we have elucidated the characteristic features of the Ti-O bonding that play an important role in dielectric properties.

§1.7 Multilevel Algorithms for Parallel Molecular Dynamics Simulations

Molecular dynamics is a powerful tool for the atomistic understanding of long-range stress-mediated phenomena, phonon properties, and mechanical failure of nanostructures. For realistic modeling of nanostructures, however, the scope of simulations must be extended to larger system sizes, longer simulated times, and more complex realism than what has been feasible until recently. Below we summarize the new multilevel algorithms we have developed.

Space-time Multiresolution Molecular Dynamics

The most prohibitive computational problem in MD simulations is associated with the Coulomb potential. Our MD algorithm is based on multiresolutions in both space and time. The long-range Coulomb interaction is computed with the fast multipole method (FMM) which reduces the computation from $O(N^2)$ to $O(N)$ for N-atom systems. Multiple time-scale (MTS) approach uses different time steps to compute forces for different interatomic separations. This multiresolution molecular dynamics (MRMD) algorithm has been implemented on parallel computers using spatial decomposition.

Multilevel Preconditioning for Variable-charge Molecular Dynamics

Conventional interatomic potential functions used in MD simulations are often fitted to bulk solid properties, and they are not transferable to systems containing defects, cracks, surfaces, and interfaces. Transferability of interatomic potentials is greatly enhanced by incorporating variable atomic charges that dynamically adapt to the local environment. Atomic charges can be determined by equalizing electronegativity. A multilevel preconditioned conjugate-gradient method is developed for this problem by splitting the Coulomb-interaction matrix into short- and long-range components. The sparse short-range matrix is used as a preconditioner to improve the spectral property of the linear system and thereby accelerating the convergence.

Wavelet-based Adaptive Curvilinear-coordinate Load Balancing

Simulation of nanostructures is often characterized by irregular atomic distribution. One practical problem in simulating such irregular systems on parallel computers is that of load imbalance. To solve this load-imbalance problem, we have developed a dynamic load-balancing scheme. In this scheme, we introduce a curvilinear coordinate system, $\vec{\xi}$, which is related to the atomic coordinate, $\vec{x}$, through the mapping, $\vec{\xi} = \vec{x} + \vec{u}(\vec{x})$. Workloads are partitioned with a uniform 3-dimensional mesh in the curvilinear coordinate system, and the load-imbalance and communication costs are minimized as a functional of $\vec{u}(\vec{x})$. Simulated annealing is used to solve the optimization problem. We apply multiresolution analysis based on wavelets to the displacement field $\vec{u}(\vec{x})$ for a compact representation of abrupt changes in partition boundaries.

Fuzzy-clustering Approach to Hierarchical, Long-time Dynamics

Many important material processes are characterized by time scales that are many orders-of-magnitude larger than atomic time scales (10^{-15} sec). A new algorithm is developed for large-scale, long-time MD simulations by combining a hierarchy of subdynamics. Global dynamics is represented by the quaternion formulation of rigid-body cluster dynamics. Fast oscillation of each atom around the local potential minimum is integrated analytically by normal-mode analysis. The residual dynamics is integrated by a symplectic, implicit integration scheme. Fuzzy clustering facilitates seamless integration of these subdynamics. The fuzzy-body/implicit-integration/normal-

mode (FIN) scheme sped up a simulation of nanocluster sintering by a factor of 28 over a conventional explicit integration scheme, without loss of accuracy.

Octree-Based Data Compression

A serious technological gap exists between the growth in processor power and that of input/output (I/O) speed. A 100-million-atom MD simulation produces 5 GBytes of data per frame, and a successful simulation project must overcome the I/O bottleneck. The large data size is also an obstacle for checkpointing simulation states for fault tolerance.

Recently we have developed a data-compression scheme for scalable I/O. We use an octree indexing and sort atoms accordingly on the resulting spacefilling curve. By storing the difference of successive atomic coordinates, the I/O requirement reduces from $O(N\log N)$ to $O(N)$. This, together with a variable-length encoding to handle outliers, reduces the I/O size from 50 to 6 Bytes/atom with a user-controlled error bound.

All of our multiresolution algorithms are highly scalable, and they have been ported to Cray T3E, SGI Origin 2000, HP Exemplar, and IBM SP computers. On a 1,024-node Cray T3E, we have achieved parallel efficiencies of 0.97 and 0.96, respectively, for a 1.02-billion-atom MD and a 20.6-million-atom variable-charge MD simulations, see Fig. 13.

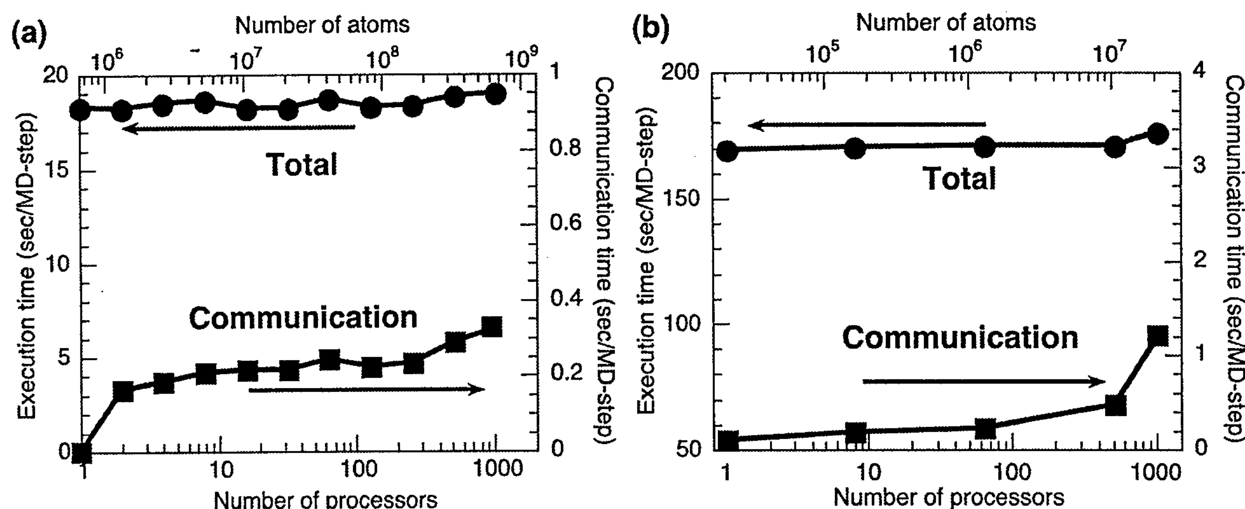

Fig. 13: Scalablity tests of (a) classical and (b) variable-charge MD algorithms on a Cray T3E computer. Total execution (circles) and communication (squares) times are plotted for 648,000P atom silica systems for classical MD and 20,160P atom alumina systems for variable-charge MD on P processors (P = 1, ..., 1,024).

§2 RESEARCH IN PROGRESS

In this section we briefly describe the simulation problems we are currently involved in.

§2.1 Stress Distribution in InAs/GaAs Mesas

The large (~ 7%) lattice mismatch and associated strain at InAs/GaAs (001) interfaces have recently been utilized to fabricate a number of nanostructures. It is well known that the strain relief leads to the formation of three-dimensional island structures above a critical amount (~ 2 monolayers) of InAs deposition. When InAs is deposited on a <100> oriented GaAs square mesa of size ~ 75 nm, however, the critical thickness for island formation is enhanced to ~ 11 ML [A. Konkar, A. Madhukar, and P. Chen, Appl. Phys. Lett. **72**, 220 (1998)]. Remarkably, this growth is "self-limiting". At the early stage of InAs deposition, In atoms migrate from the side walls to the mesa top, realizing the substrate encoded size-reducing epitaxy (SESRE). Once the InAs thickness on the mesa top reaches ~ 11 ML, however, In atoms migrate away from the mesa top. A possible mechanism of the migration-direction reversal is the built-up strain energy in the InAs film and the

associated change in the stress-gradient direction. More recently, parallel chains of InAs islands have been fabricated on top of $[1\bar{1}0]$ oriented stripe mesas of sub-100-nm widths on GaAs (001) substrates.

Our ongoing simulation effort focuses on understanding atomic level stress distributions relevant to the self-limited nature of lattice-mismatched overlayer growth of InAs on GaAs. This is of considerable significance to realizing fault-tolerant, high density, two- and three-dimensional arrays of quantum boxes for applications in anticipated new paradigms for information technology in the 21st century.

Large-scale MD simulations are performed to investigate the mechanical stresses on InAs/GaAs nanomesas with {101}-type sidewalls, see Fig. 14. The in-plane lattice constant of InAs layers parallel to the InAs/GaAs(001) interface starts to exceed the InAs bulk value at 12 ML and the hydrostatic stresses in InAs layers are tensile above 12th ML. As a result, it is not favorable to have InAs overlayers thicker than 12 ML. This may explain the experimental findings of the growth of flat InAs overlayers with self-limiting thickness of ~ 11 ML on GaAs nanomesas.

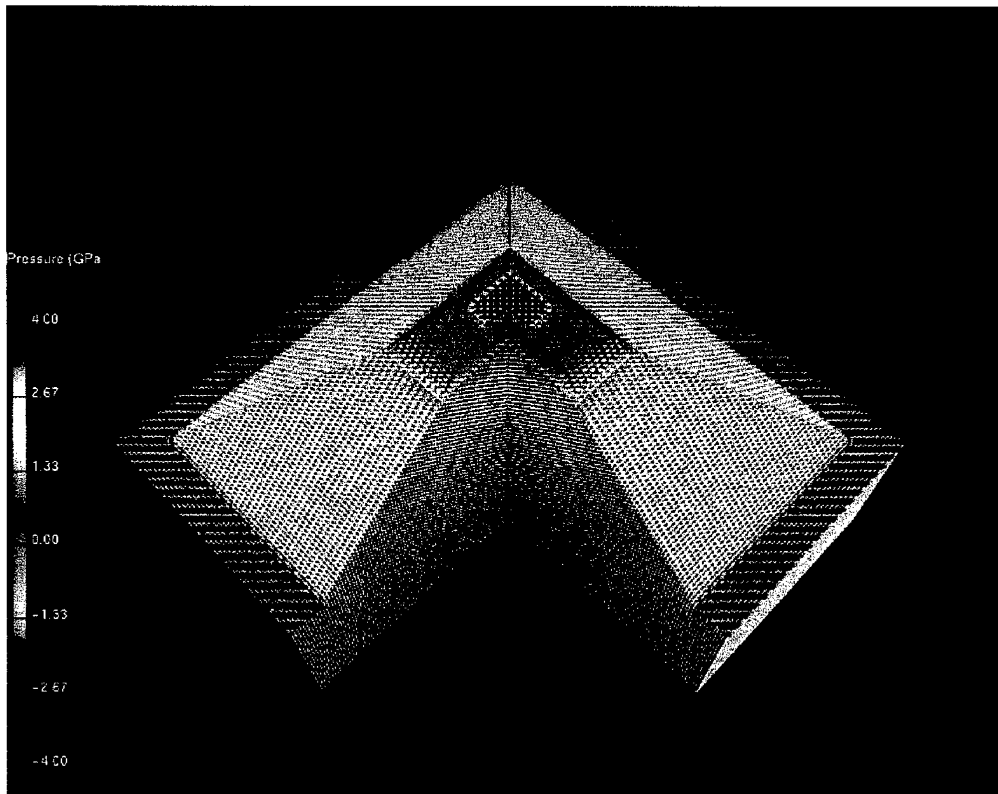

Fig. 14: Atomic-level hydrostatic pressure distribution in an InAs/GaAs square mesa with a 12 ML InAs overlayer. Negative pressure means tensile and positive pressure means compressive.

§2.2 NANOINDENTATION IN Si_3N_4 SURFACES

Nanoindentation testing is a unique local probe of mechanical properties of materials at surfaces and multilayered structures. This technique is especially useful in testing surfaces and thin films in microelectronics industry. For example, it is used for measuring critical stresses for dislocation generation in semiconductor devices. The importance of atomic-level understanding of indentation processes is widely recognized.

Using MD simulations, we are investigating nanoindentation in Si_3N_4. The nanoindentation simulation is performed on the (0001) surface of a 60 nm × 60 nm × 30 nm crystalline α-Si_3N_4 slab

consisting of 10 million atoms, see Fig. 15. The sample is indented using a pyramid indenter with a load ~ 10 μN and indentation depth ~ 10 nm. From the load-displacement curve, hardness value is estimated to be of 50.3 GPa. (We have also calculated the hardness of amorphous Si_3N_4 to be 31.5 GPa using a similar geometry.) Our simulations reveal significant plastic deformation and pressure-induced amorphization under the indenter. The simulations also exhibit anisotropic fracture toughness: Indentation cracks are observed along the $[\bar{1}2\bar{1}0]$ direction, which coincides with one of the diagonal directions of the indenter, but not for the other diagonal direction, $[1\bar{1}00]$.

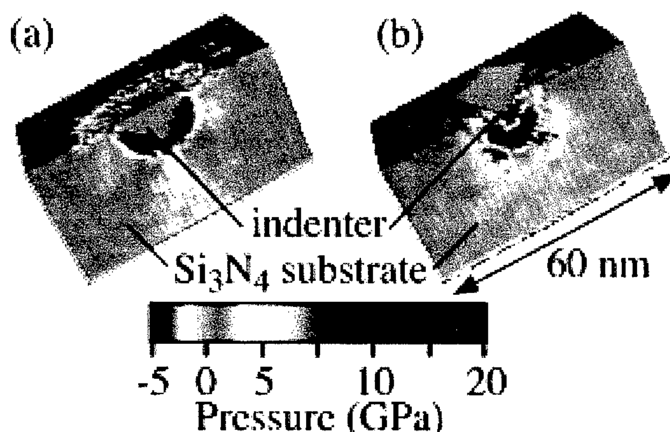

Fig. 15: Pressure distribution in Si_3N_4 during (a) loading and (b) unloading of a nanoindenter.

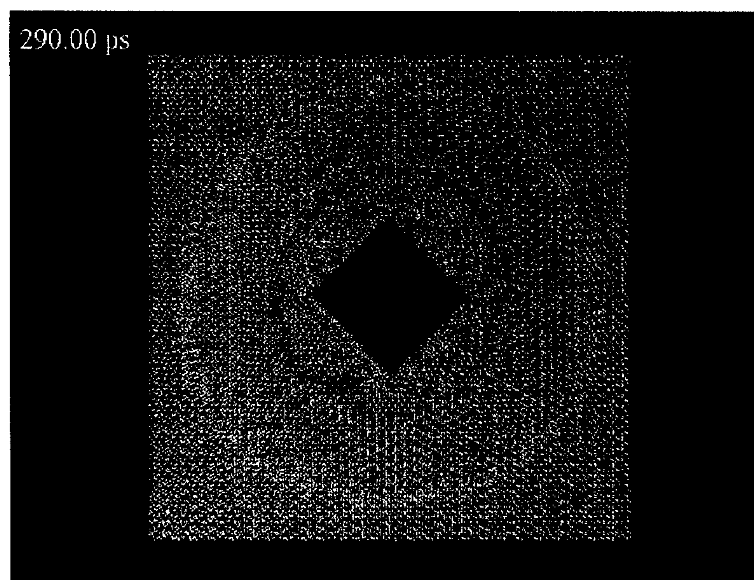

Fig. 16: Top view of the atomic distribution in a Si_3N_4 (0001) surface after unloading of a nanoindenter.

§2.3 Scalable Molecular-Dynamics/Quantm-Mechanical Algorithms

Having established scalable MD algorithms, current focus of research is how to enhance the physical realism of these simulations. A more accurate but compute-intensive method explicitly deals with electron wave functions and their mutual interactions in the framework of the density functional theory (DFT) and electron-ion interaction using pseudopotentials. (The DFT, for the development of which Walter Kohn received a 1998 Nobel chemistry prize, reduces the exponentially complex quantum N-body problem to a self-consistent $O(N^3)$ eigenvalue problem.)

Our DFT code is based on the minimization of an energy functional in the local density approximation and uses a higher-order finite-difference method with pseudopotentials. Space is discretized with a grid of regular spacing, and the kinetic-energy operator is expanded up to sixth order for higher-order finite-difference expansion. To further speed up the convergence, we have used a multigrid acceleration scheme. Atomic forces are calculated according to the Hellmann-Feynman theorem.

We have also implemented an $O(N)$ DFT scheme on parallel computers. This scheme computes the sparse density matrix with which physical quantities such as the energy and forces are calculated. This algorithm uses higher-order finite differencing, nonlocal pseudopotentials, representation of the density matrix with local nonorthogonal orbitals, and spatial decomposition for parallelization. We have implemented the $O(N)$ approach for GaAs systems containing up to 22,500 atoms on 1,024 T3E nodes, see Fig. 17.

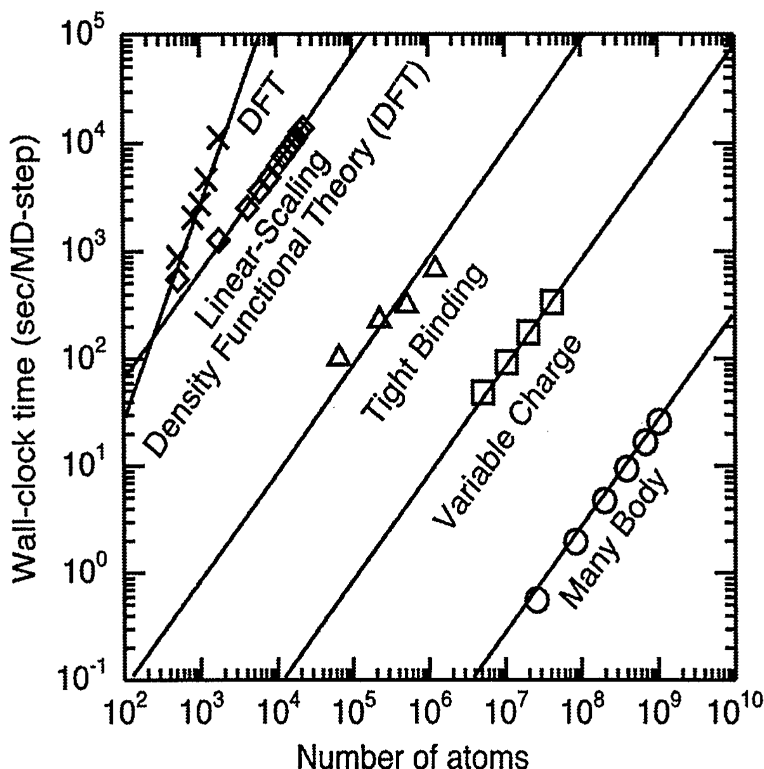

Fig. 17: Performance of linear-scaling MD and QM simulation algorithms on 1,024 Cray T3E processors: classical MD (circles); environment-dependent, variable-charge MD approach (squares); QM scheme based on the tight-binding method (triangles); and self-consistent QM scheme based on the density-functional theory (diamonds). The conventional $O(N^3)$ density-functional algorithm is also shown (crosses).

§2.3 Hybrid Molecular-Dynamics/Quantm-Mechanical Simulation Approach

We have also developed scalable software infrastructure to enable multiscale simulations of nanoelectronic devices using MD and QM methods, see Fig. 18.

In the hybrid QM/MD simulation scheme, a quantum mechanical system described by the density functional theory on real-space multigrids is embedded in a classical system of atoms interacting via an empirical interatomic potential. Handshake atoms coupling the quantum and the classical systems are treated by a novel scaled position method. The scheme is implemented on parallel computers using both task and spatial decompositions. An application to oxidation of Si (100) surface demonstrates seamless coupling of the quantum and the classical systems.

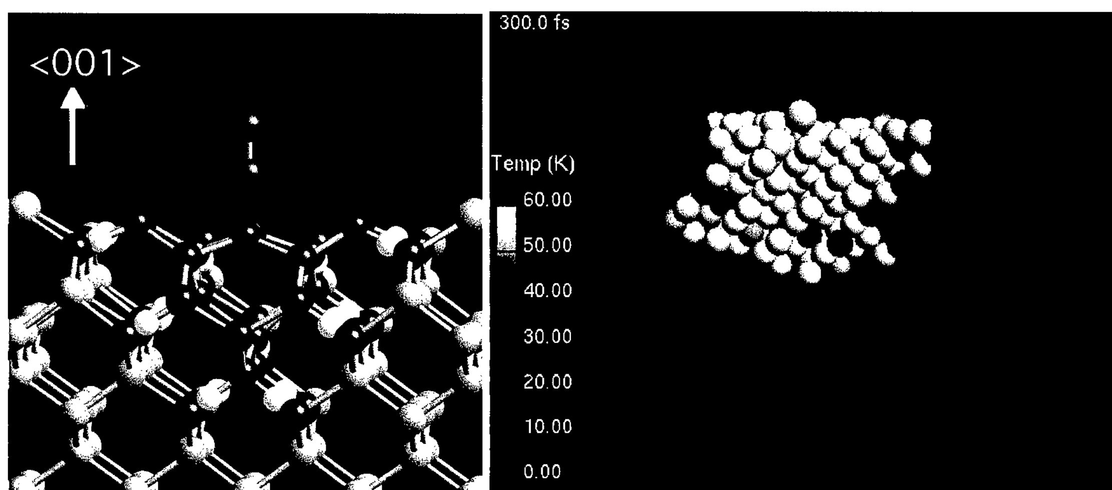

Fig. 18: (Left) Hybrid QM/MD simulation of an O_2 molecule (green) on a Si(001) surface. The O and magenta Si atoms are treated quantum mechanically. Handshake atoms (yellow) are placed between the QM and nearest-neighbor MD (blue) Si atoms. (Right) Upon the dissociation of the O_2 molecule, enormous heat is transmitted through the QM/MD boundary into the MD region.

§3 INTERACTIONS

Below we briefly describe the interactions we have had with researchers at government laboratory industry, and university.

Argonne National Laboratory: We are collaborating with a number of scientists at the DOE's Argonne National Laboratory in Illinois. One of our students, Alok Chatterjee, has conducted neutron scattering measurements of structures and phonons in nanocluster-assembled SiC with Dr. C. Loong at the Intense Pulsed Neutron Source Division. We are also collaborating with Drs. T. Disz, W. Gropp, R. Stevens, and M. Papka on designing immersive and interactive visualization tools, parallel algorithms, and message-passing.

NASA: We are collaborating with Dr. S. Saini at NASA Ames on algorithm design and implementation of large-scale materials simulations on NASA's Information Power Grid.

Intel: We have ongoing collaboration on atomistic simulation of electronic devices with Dr. S. Shankar's simulation and modeling group at Intel.

Motorola: Recently we have started collaboration on sintering of multilayered ceramic films with Dr. D. Wilcox's experimental group at Ceramic Technology Center at Motorola.

University of Southern California: We have been collaborating with Dr. A. Madhukar's group at the University of Southern California on intelligent manufacturing of electronic devices.

§4 TRAINING OF GRADUATE STUDENTS

Our graduate students are enrolled in a unique, multidisciplinary program that allows them to obtain a Ph.D. in physics and an MS from the Department of Computer Science. The aim of this program is to provide students with broad-based training in high performance computing and communications (HPCC) and the physical sciences. In connection with this program, we have introduced a number of HPCC courses in the Physics and Computer Science Departments. The Department of Physics has two graduate courses in computational physics that are cross-listed with computer science courses. The first course deals with classical and quantum simulations on parallel architectures. The second course, designed for advanced graduate students, covers special topics such as multiscale phenomena, multigrid methods, wavelets, *etc.* In the Department of Computer Science, we have introduced three new HPCC courses. Soon two more courses will be added to the

computer-science curriculum: a) Grid Computing; and b) Scientific Visualization. The courses we have introduced emphasize parallel computing and algorithm design for large-scale scientific applications. Students have access to a number of parallel machines to gain hands-on experience and to perform research on large-scale computational projects.

Our students have excellent opportunities to broaden their research experience beyond the traditional university based environment. They are involved in our collaborative efforts with computational and experimental scientists at government laboratories, industries, and other universities. These interactions have significantly enhanced the research capabilities of students. Through these contacts, students also have access to excellent parallel computing and visualization facilities at other institutions.

One of the dual-degree students, Dr. Alok Chatterjee, supervised by the PIs of this program received a prestigious Enrico Fermi Fellowship from the US Department of Energy in 1999. For the development of the dual-degree program, Rajiv K. Kalia and Aiichiro Nakano have received a Distinguished Faculty Award and a Faculty Excellence Award, respectively, from LSU in 1999.

§5 COMPUTATIONAL FACILITIES

For the research program, our Concurrent Computing Laboratory for Materials Simulations (*CCLMS*) at Louisiana State University (LSU) has two parallel computing laboratories, one in the Department of Physics and Astronomy and the other in the Department of Computer Science. With $3 million in infrastructure enhancement grants from the State of Louisiana, these labs have been equipped with several parallel machines including: **Digital Alpha cluster**—64 Alpha processors connected via Gigaswitches; **PC cluster**—100 PCs (550 MHz Pentium III, to be upgraded to a 164-node PC cluster with 733 MHz processors) linked by fast ethernet switches (Fig. 19); **systolic architecture**—a 64-cell Intel iWarp.

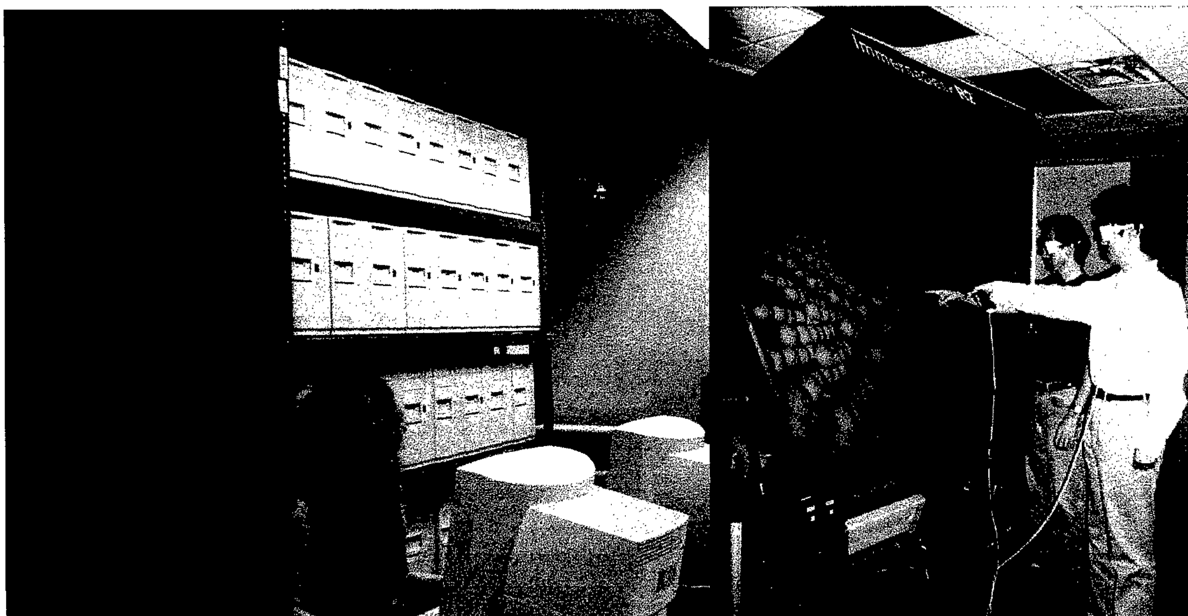

Fig. 19 : (Left) A 100-node PC cluster at the *CCLMS* . (Right) *ImmersaDesk* virtual environment at the *CCLMS* .

We have also established a virtual environment (VE) laboratory that features an interactive and immersive *ImmersaDesk* for visualization (Fig. 19). The VE lab also has a multiprocessor SGI Onyx2/InfiniteReality2, an Octane/MXE, and an 8-processor Power Center graphics servers as well as a number of SGI graphics workstations. Via high-speed networks, the *ImmersaDesk* is fully integrated with the existing parallel machines at the *CCLMS* and with massively parallel computers

at national computer centers. (A recent NSF high performance connectivity award to LSU allows access to high-speed backbone networks.)

Simulations have also been performed on Cray T3E, SGI Origin 2000, and IBM SP computers at DoD's Major Shared Resource Centers and a Hewlett Packard/Convex Exemplar at the Center for Advanced Computing Research at Caltech.

§6 PUBLICATIONS

1. "Role of ultrafine microstructures in dynamic fracture in nanophase silicon nitride," R. K. Kalia, A. Nakano, A. Omeltchenko, K. Tsuruta, and P. Vashishta, Phys. Rev. Lett. **78**, 2144 (1997).
2. "Crack front propagation and fracture in a graphite sheet: a molecular-dynamics study on parallel computers," A. Omeltchenko, J. Yu, R. K. Kalia, and P. Vashishta, Phys. Rev. Lett. **78**, 2148 (1997).
3. "An adaptive curvilinear-coordinate approach to dynamic load balancing of parallel multi-resolution molecular dynamics," A. Nakano and T. Campbell, Parallel Comput. **23**, 1461 (1997).
4. "Parallel multilevel preconditioned conjugate-gradient approach to variable-charge molecular dynamics," A. Nakano, Comput. Phys. Commun. **104**, 59 (1997).
5. "Fuzzy clustering approach to hierarchical molecular dynamics simulation of multiscale materials phenomena," A. Nakano, Comput. Phys. Commun. **105**, 139 (1997).
6. "Fracture in silicon nitride and alumina thin films," T. J. Campbell, A. Nakano, A. Omeltchenko, R. K. Kalia, and P. Vashishta, Mat. Res. Soc. Symp. Proc. **446**, 163 (1997).
7. "Fracture of nanophase ceramics: A molecular dynamics study," A. Nakano, R. K. Kalia, A. Omeltchenko, K. Tsuruta, and P. Vashishta, Mat. Res. Soc. Symp. Proc. **457**, 187 (1997).
8. "Structure, mechanical properties, and dynamic fracture in nanophase silicon nitride via parallel molecular dynamics," K. Tsuruta, A. Omeltchenko, A. Nakano, R. K. Kalia, and P. Vashishta, Mat. Res. Soc. Symp. Proc. **457**, 205 (1997).
9. "Multilevel algorithms for large-scope molecular dynamics simulations of nanostructured materials on parallel computers," A. Nakano, in *Proceedings of the ASCI (Advanced School for Computing and Imaging) 97* Conference, edited by H. E. Bal, H. Corporaal, P. P. Jonker, J. F. M. Tonino (Heijen, Netherlands, 1997) p. 121.
10. "Multimillion-atom molecular dynamics simulation of atomic level stresses in Si(111)/Si_3N_4(0001) nanopixels," M. E. Bachlechner, A. Omeltchenko, A. Nakano, R. K. Kalia, P. Vashishta, I. Ebbsjö, A. Madhukar, and P. Messina, Appl. Phys. Lett. **72**, 1969 (1998).
11. "Dynamics of consolidation and crack growth in nanocluster-assembled amorphous silicon nitride," K. Tsuruta, A. Nakano, R. K. Kalia, and P. Vashishta, J. Am. Ceram. Soc. **81**, 433 (1998).
12. "Multilevel algorithms for large-scope molecular dynamics simulations of nanostructures on parallel computers," A. Nakano, R. K. Kalia, and P. Vashishta, VLSI Design **8** (1-4), 123 (1998).
13. "Atomistic simulation of nanostructured materials using parallel multiresolution algorithms," A. Nakano, M. E. Bachlechner, T. J. Campbell, R. K. Kalia, A. Omeltchenko, K. Tsuruta, P. Vashishta, S. Ogata, I. Ebbsjö, and A. Madhukar, IEEE Comput. Sci. Eng. **5** (4), 68 (1998).
14. "Oxidation dynamics of nanophase aluminum clusters: A molecular dynamics study," S. Ogata, T. J. Campbell, K. Tsuruta, A. Nakano, R. K. Kalia, P. Vashishta, and C.-K. Loong, Mat. Res. Soc. Symp. Proc. **481**, 625 (1998).

15. "Multimillion atom molecular dynamics simulations of ceramic materials and interfaces on parallel computers," P. Vashishta, M. E. Bachlechner, R. K. Kalia, A. Nakano, A. Omeltchenko, K. Tsuruta, I. Ebbsjö, and A. Madhukar, in *Proceedings of the Special Symposium on Advanced Materials*, edited by T. Imura, H. Fujita, T. Ichinokawa, and H. Kawazoe (Nagoya, Japan, 1998) p. 47.

16. "Structure and mechanical failure in nanophase silicon nitride: Large-scale molecular-dynamics simulations on parallel computers," A. Omeltchenko, A. Nakano, K. Tsuruta, R. K. Kalia, and P. Vashishta, in *Advances in Metal and Semiconductor Clusters Vol. IV: Cluster Materials*, edited by M. Duncan (JAI Press, Stamford, CN, 1998) p. 263.

17. "Structural correlations and mechanical behavior in nanophase silica glasses," T. Campbell, R. K. Kalia, A. Nakano, F. Shimojo, K. Tsuruta, and P. Vashishta, Phys. Rev. Lett. **82**, 4018 (1999).

18. "Dynamics of oxidation of aluminum nanoclusters using variable charge molecular-dynamics simulations on parallel computers," T. Campbell, R. K. Kalia, A. Nakano, P. Vashishta, S. Ogata, and S. Rodgers, Phys. Rev. Lett. **82**, 4866 (1999).

19. "Variable-charge interatomic potentials for molecular-dynamics simulations of TiO_2," S. Ogata, H. Iyetomi, K. Tsuruta, F. Shimojo, R. K. Kalia, A. Nakano, and P. Vashishta, J. Appl. Phys. **86**, 3036 (1999).

20. "Parallel molecular dynamics simulations of high temperature ceramics," A. Chatterjee, T. Campbell, R. K. Kalia, A. Nakano, A. Omeltchenko, K. Tsuruta, and P. Vashishta, J. Euro. Ceram. Soc. **19**, 2257 (1999).

21. "Structural correlations at Si/Si_3N_4 interface and atomic stress in Si/Si_3N_4 nanopixels--10 million-atom molecular dynamics simulation on parallel computers," M. E. Bachlechner, R. K. Kalia, A. Nakano, A. Omeltchenko, P. Vashishta, I. Ebbsjö, A. Madhukar, and G.-L. Zhao, J. Euro. Ceram. Soc. **19**, 2265 (1999).

22. "Multiresolution load balancing in curved space: the wavelet representation," A. Nakano, Concurrency: Practice and Experience **11**, 343 (1999).

23. "A rigid-body based multiple time-scale molecular dynamics simulation of nanophase materials," A. Nakano, Int. J. High Performance Comput. Appl. **13**, 154 (1999).

24. "Dynamic fracture analysis," P. Vashishta and A. Nakano, Comput. Sci. Eng. **1** (5), 20 (1999).

25. "Scalable molecular-dynamics, visualization, and data-management algorithms for materials simulations," A. Nakano, R. K. Kalia, and P. Vashishta, Comput. Sci. Eng. **1** (5), 39 (1999).

26. "Large-scale atomistic simulation of dynamic fracture," P. Vashishta, R. K. Kalia, and A. Nakano, Comput. Sci. Eng. **1** (5), 56 (1999).

27. "Pressure induced structural transformation in nanocluster assembled gallium arsenide," S. Kodiyalam, A. Chatterjee, I. Ebbsjö, R. K. Kalia, H. Kikuchi, A. Nakano, J. P. Rino, and P. Vashishta, Mat. Res. Soc. Symp. Proc. **536**, 545 (1999).

28. "Molecular dynamics simulations of nanoindentation of silicon nitride," P. Walsh, A. Omeltchenko, H. Kikuchi, R. K. Kalia, A. Nakano, and P. Vashishta, Mat. Res. Soc. Symp. Proc. **539**, 119 (1999).

29. "Dynamic fracture in nanophase ceramics and diamond films: Multimillion atom parallel molecular-dynamics simulations," A. Omeltchenko, K. Tsuruta, A. Nakano, R. K. Kalia, P. Vashishta, O. Shenderova, in *Computer-Aided Design of High-Temperature Materials*, edited by A. Pechenik, R. K. Kalia, and P. Vashishta (Oxford Univ. Press, Oxford, 1999) p. 81.

30. "Structure and dynamics of consolidation and fracture in nanophase ceramics via parallel molecular dynamics," K. Tsuruta, J. Wang, A. Omeltchenko, A. Nakano, R. K. Kalia, and P.

Vashishta, in *Computer-Aided Design of High-Temperature Materials*, edited by A. Pechenik, R. K. Kalia, and P. Vashishta (Oxford Univ. Press, Oxford, 1999) p. 323.

31. "Structural correlations in amorphous SiO_2 at high pressures," J. P. Rino, A. Nakano, R. K. Kalia, and P. Vashishta, in *Computer-Aided Design of High-Temperature Materials*, edited by A. Pechenik, R. K. Kalia, and P. Vashishta (Oxford Univ. Press, Oxford, 1999) p. 374.

32. "Multilevel algorithms for computational high-temperature materials research," A. Nakano, T. Campbell, R. K. Kalia, and P. Vashishta, in *Computer-Aided Design of High-Temperature Materials*, edited by A. Pechenik, R. K. Kalia, and P. Vashishta (Oxford Univ. Press, Oxford, 1999) p. 422.

33. "Multimillion atom molecular dynamics simulations of glasses and ceramic materials," P. Vashishta, R. K. Kalia, and A. Nakano, in *Physics of Glasses: Structure and Dynamics*, edited by P. Jund and R. Jullien (American Institute of Physics, Melville, NY, 1999) p. 149.

34. "Stress domains in Si(111)/Si_3N_4(0001) nanopixel - 10 million-atom molecular dynamics simulations on parallel computers," A. Omeltchenko, M. E. Bachlechner, A. Nakano, R. K. Kalia, P. Vashishta, I. Ebbsjö, A. Madhukar, and P. Messina, Phys. Rev. Lett. **84**, 318 (2000).

35. "Dislocation emission at silicon/silicon nitride interface - a million atom molecular dynamics simulation on parallel computers," M. E. Bachlechner, A. Omeltchenko, A. Nakano, R. K. Kalia, P. Vashishta, I. Ebbsjö, A. Madhukar, Phys. Rev. Lett. **84**, 322 (2000).

36. "Molecular dynamics simulation of pressure induced structural transformation in silicon carbide," F. Shimojo, I. Ebbsjö, R. K. Kalia, A. Nakano, J. P. Rino, and P. Vashishta, Phys. Rev. Lett. **84**, 3338 (2000).

37. "Topology of amorphous gallium arsenide on intermediate length scales: a molecular dynamics study," I. Ebbsjö, R. K. Kalia, A. Nakano, J. P. Rino, and P. Vashishta, J. Appl. Phys. **87**, 7708 (2000).

38. "Multiresolution algorithms for massively parallel molecular dynamics simulations of nanostructured materials," R. K. Kalia, T. J. Campbell, A. Chatterjee, A. Nakano, P. Vashishta, and S. Ogata, Comput. Phys. Commun. **128**, 245 (2000).

39. "Multimillion atom simulations of nanostructured materials on parallel computers - sintering and consolidation, fracture, and oxidation," P. Vashishta, M. E. Bachlechner, T. J. Campbell, R. K. Kalia, H. Kikuchi, S. Kodiyalam, A. Nakano, S. Ogata, F. Shimojo, and P. Walsh, Prog. Theor. Phys. Suppl. **138**, 175 (2000)

40. "Large-scale atomistic modeling of nanoelectronic structures," A. Nakano, M. E. Bachlechner, P. Branicio, T. J. Campbell, I. Ebbsjö, R. K. Kalia, A. Madhukar, S. Ogata, A. Omeltchenko, J. P. Rino, F. Shimojo, P. Walsh, and P. Vashishta, IEEE Trans. Electron Dev., in press.

41. "Scalable I/O of large-scale molecular-dynamics simulations: a data-compression algorithm," A. Omeltchenko, T. J. Campbell, R. K. Kalia, X. Liu, A. Nakano, and P. Vashishta, Comput. Phys. Commun., in press.

42. "A scalable molecular-dynamics-algorithm suite for materials simulations: design-space diagram on 1,024 Cray T3E processors," F. Shimojo, T. J. Campbell, R. K. Kalia, A. Nakano, P. Vashishta, S. Ogata, and K. Tsuruta, Future Generation Comput. Sys., in press.

43. "Hybrid quantum mechanical/molecular dynamics simulation on parallel computers: density functional theory on real-space multigrids," S. Ogata, F. Shimojo, A. Nakano, P. Vashishta, and R. K. Kalia, Comput. Phys. Commun., to appear.

44. "Large-scale atomistic simulation of nanostructured materials on parallel computers," P. Vashishta, M. E. Bachlechner, T. J. Campbell, R. K. Kalia, H. Kikuchi, S. Kodiyalam, A. Nakano, S. Ogata. F. Shimojo, and P. Walsh, in *Phase Transformations and Evolution in*

Materials, edited by P. E. A. Turchi and T. Gonis (The Minerals, Metals & Materials Society, Warrendale, PA, 2000) to appear.

45. "Multi-million atom molecular-dynamics simulations of stresses in Si(111)/a-Si_3N_4 nanopixels," M. E. Bachlechner, A. Omeltchenko, P. Walsh, A. Nakano, R. K. Kalia, P. Vashishta, I. Ebbsjö, and A. Madhukar, Mat. Res. Soc. Symp. Proc., to appear.

46. "Multimillion-atom simulations of atomic-level surface stresses and migration processes on InAs/GaAs mesas," X. Su, R. K. Kalia, A. Madhukar, A. Nakano, and P. Vashishta, Mat. Res. Soc. Symp. Proc., to appear.

§7 SCIENTIFIC PERSONNEL

Three faculty members (Aiichiro Nakano, Rajiv K. Kalia, and Priya Vashishta) are involved in the research projects described in §1 and §2. A PostDoc, Dr. Sanjay Kodiyalam, has studied the structural transformation of GaAs nanocrystals, and another PostDoc, Dr. Hideaki Kikuchi, has developed scalable MD algorithms and studied the fracture of GaAs. Several visiting professors have also collaborated with us on this project: Dr. Ingvar Ebbsjö of Studsvik Neutron Research Laboratory at Univ. of Uppsala in Sweden has worked on the development of interatomic potentials; Dr. Shuji Ogata of Yamaguchi Univ. in Japan has developed a parallel variable-charge MD simulation code and studied the oxidation dynamics of Al nanoclusters; Dr. Jose Rino of Federal Univ. of Sao Carlos in Brazil is working with us on MD simulations of SiO_2 and GaAs/InAs heterostructures.

Award/Honor

A Faculty Early Career Development (CAREER) Award (1997-2001) has been awarded to Aiichiro Nakano by the Division of Advanced Scientific Computing of National Science Foundation. This CAREER project is developing an integrated research and educational framework in high performance computing and communications (HPCC), and it has provided well-trained graduate students in HPCC needed for this DEPSCoR program.

§8 INVENTIONS

None.